GeoResJ 7 (2015) 14–21

Contents lists available at ScienceDirect

GeoResJ

journal homepage: www.elsevier.com/locate/GRJ

Non-tidal loading by the Baltic Sea: Comparison of modelled deformation with GNSS time series

M. Nordman *, H. Virtanen, S. Nyberg, J. Mäkinen

Finnish Geospatial Research Institute (FGI), National Land Survey of Finland, Masala, Finland

ARTICLE INFO

Article history:
Received 3 November 2014
Revised 25 February 2015
Accepted 10 March 2015
Available online 31 March 2015

Keywords:
Satellite geodesy
Geodynamics
Baltic Sea
Non-tidal loading

ABSTRACT

We study the influence of non-tidal loading by the Baltic Sea on GNSS daily coordinate time series. The momentary sea surface is estimated from hourly tide gauge recordings around the Baltic and the load is convolved with Green's functions to determine 3-D deformation, gravity, potential and tilt effects at 193 stations around the Baltic. This paper concentrates on 3-D deformation at a small number of continuous GNSS stations. Daily coordinate time series based on both Precise Point Positioning (PPP) and double differences (DD) were used. We find that for the east component of inter-station vectors crossing the Baltic, up to 56% of the variance can be explained by the Baltic loading. In the north and up components the Baltic loading is not well detectable. We think that for the north component this is due to station positions, and for the up component also to interaction with regional atmospheric loading.

1. Introduction

The loading effects of ocean tides are nowadays routinely removed from GNSS measurements, typically using the recommendations of the International Earth Rotation and Reference Systems Service (IERS) conventions [22]. In recent years there has been increased interest of the effects of the non-tidal variation in ocean loading. This concerns both the "normal" ocean circulation (e.g. [17-19,24,29] and special occasions like storm surges [12,13,17].

The variations in the sea level can be abrupt and large, for example during storms. The variable load may cause significant effects in geodetic measurements, especially near the coastline. This may cause problems in time-lapse measurements (e.g. GNSS campaigns, absolute gravity measurements) as well as in continuous time series. In GNSS time series 40% of the variation can be due to varying atmospheric, hydrological and ocean masses [9], which in turn makes the derived rate uncertainties larger than expected [6,7].

The seasonal loading signals, while typically smaller in size may distort the trend estimation, especially in shorter time series. This has been studied using daily [18,29], weekly [24] and monthly [7,19] time series of GNSS.

Most of the papers mentioned above treat vertical deformation only. The exception is Geng et al. [13] who detect the 3-D deformation during a storm surge event in the North Sea, with sub-daily resolution. We study the 3-D effect of the Baltic Sea loading in daily time series of GPS derived positions, but we have a time series of 1.5 years, which includes longer-period phenomena than the one-month time series of Geng et al. [13].

The relevant quantity for load calculations in ocean areas is the ocean bottom pressure (OBP), i.e. the sum of the load by the water column and the atmospheric pressure on the sea surface. However, in this study we are going to neglect the atmospheric pressure part. Can anything useful come out from such a computation?

Suppose that the atmospheric surface pressure anomaly is regionally near-uniform, i.e. it produces a near-uniform vertical deformation and near-zero horizontal deformations. When we then calculate the loading effect by the sea using only the water column part of the OBP, what comes out is not the total deformation but the deviation of the deformation from the regional common mode. The common mode in the GPS-derived coordinates can be eliminated by differencing. At the same time we difference the load corrections. Thus the Baltic loading could be studied using the differences, without knowledge of the common atmospheric mode. Note that the differencing also in part eliminates other regional common modes, like the annual hydrological load cycle.

The success of this approach obviously depends on the validity of the common-mode assumption. It will turn out that this assumption works for short vectors and horizontal deformation, and fails for long vectors and vertical deformation. While we

* Corresponding author at: Finnish Geospatial Research Institute FGI, Geodeetinrinne 2, FI-02430 Masala, Finland. Tel.: +358 40 661 6678.
E-mail address: maaria.nordman@nls.fi (M. Nordman).

http://dx.doi.org/10.1016/j.grj.2015.03.002
2214-2428/

neglect the atmospheric contribution to Baltic OBP in this study, we point out that this makes it easy to rigorously superpose our Baltic deformation results on atmospheric load calculations that use a neutral response of the Baltic instead of any inverse barometer type of behavior [15,31].

In what follows, we compute the loading effect of the Baltic Sea level variations using hourly sea level surfaces. We then difference both the computed deformation and the coordinate changes measured by GPS at selected station pairs around the Baltic Sea and compare them. We use two different daily time series of GPS-derived positions: the PPP (Precise Point Positioning) time series provided by the Jet Propulsion Laboratory and a double difference solution computed at the Finnish Geodetic Institute (FGI). The data and methods are described in Sections 2 (Baltic) and 3 (GPS). In the fourth section are the results of the loading and GPS comparison, fifth section contains the discussion and the last section is left for the conclusions and outlook.

2. Baltic Sea

The Baltic Sea is a well-monitored semi-enclosed sea in northern Europe. The level of the Baltic Sea level has been studied and recorded since 18th century (e.g. [10,20]). Nowadays a dense network of tide gauges monitors the Baltic Sea continuously and automatically, and also the satellite altimetry missions provide observations on the region. Thus, the Baltic Sea is suitable for testing and studying the effect of mass variations. The Baltic Sea water storage has been compared to GRACE analysis [26] and the mass variations and loading have been studied using gravimeters (e.g. [21,25] and GPS [19].

The mass variations of the Baltic Sea are mostly due to atmospheric pressure changes and wind, which redistribute the water within the basin and also govern the water exchange with the North Sea which determines the so-called fill level of the Baltic. Because the connection to the North Sea is via the narrow Danish Straits, the tides are small and the effect of local variations due to wind conditions is large.

Fig. 1 shows the magnitudes of 3D loading deformation calculated for a one by one degree grid. The load is a uniform fill level: one meter layer of water. The calculation methods are described in Section 2.2. The maximum vertical deformation near Gotland Island is about –21 mm and the horizontal maximums are about 4 mm. A variation in uniform fill level is in fact very close to the first Empirical Orthogonal Function (EOF) of Baltic Sea mass variation as determined by Wiehl et al. [28].

2.1. Sea level heights and surfaces

Previous studies of non-tidal ocean loading (e.g. [29]) typically rely on oceanographic models to estimate the load. However, in the Baltic we have a unique opportunity to estimate the momentary sea level directly from the more that 60 tide gauges that surround the sea at all coasts and provide hourly data in near real time through the Baltic Operational Oceanographic Service (BOOS, http://boos.org). We supplemented the BOOS data with Finnish tide gauges from the Finnish Meteorological Institute FMI. The hourly sea level surfaces were then created by interpolating between the hourly sea level heights at the tide gauges. Minimum-curvature-surface splines (routines in the IDL software library http://www.exelisvis.com/ProductsServices/IDL.aspx) were used. The number of tide gauges available varies in the computation. The data is near real-time and thus may suffer from gaps in data stream. The number of stations used in the interpolation varies from 40 to 60 stations. As the sea level is typically a rather smooth surface, this variation in the support points used does not appreciably influence the surface models created. The use of tide gauges instead of models is discussed in Section 5.

Steric effects are neglected in this preliminary study. The steric effects are primarily seasonal and about a one order of magnitude less than the effects in the variation of the water volume [26]. The tides in the Baltic Sea are only few centimetres in most areas and maximally 0.2 m (in the extremity of the Gulf of Finland). The tidal variation in the sea level is interpolated by our spline-interpolation between the tide gauges in the same way as the non-tidal variation.

2.2. Calculation of loading deformation

The sea surface derived from tide gauges, sampled at 0.2 × 0.1 degrees resolution (longitude × latitude) over the Baltic and coasts provides the model grid for the deformation calculation. The load response was computed using the program set SPOTL [1]. Green's functions for the Gutenberg–Bullen Earth model A (as described in [11]) are used. SPOTL overlays the land/sea mask on the model grid and resamples it to a new radial load grid centered on the computation point. The resolution for the coastline is 1/64 of degree. SPOTL also provides densities of surface sea water from the World Ocean Atlas [2]. In the Baltic they are typically 1003–1004 kg m^{-3}, though for the present purposes the calculation could just as well be made with nominal density values (say 1000 or 1027 kg m^{-3}).

The computation produces gravity change, potential change, deformation in three dimensions, tilt deformation in north and south and strain in north, east and shear. The center of mass of the solid Earth (CE) reference frame was chosen for the computation.

We have computed hourly time series for 193 stations in Fennoscandia, Baltic countries and on the south coast of the Baltic Sea. The time period is 27.2.2008–31.12.2012. Fig. 2 shows all components computed in the run for a single station. The output are hourly values (black in Fig. 2). For the comparison with GNSS time series daily values were computed (green in Fig. 2).

3. GNSS time series

We have used two types of GPS-derived coordinate time series. The first one has been computed at Jet Propulsion Laboratory (JPL, ftp://sideshow.jpl.nasa.gov/pub/JPL_GPS_Timeseries/repro2011b/post/point/, 8.3.2013), hereafter referred to as JPL time series. These time series are computed with Precise Point Positioning method using GIPSY-OASIS II software [32] fixing ambiguities [4]. While the preliminary products are non-fiducial, the daily results are transformed to IGS08. (http://sideshow.jpl.nasa.gov/post/tables/GPS_Time_Series.pdf). This is a global transformation; as such it could mask and smear regional loading phenomena in the coordinate time series, but not in the difference time series in a limited area which is what we are working with. These data are available for the whole period of Baltic Sea loading (February 2008 until end of 2012). Due to gaps and spikes in time series we have chosen a period of 671 days, starting in February 2008 and ending in December 2009.

The second time series has been computed at the Finnish Geodetic Institute (FGI, now Finnish Geospatial Research Institute FGI) using double differences and the Bernese GPS Software version 5.0 [8], hereafter referred as FGI time series. The original time series were produced for a regional test survey, and in that application the daily results were transformed to ITRF2008. Now this regional transformation could severely smear and mask the deformation signals we are looking for, even in the station differences. We therefore took the daily normal equations and instead of the

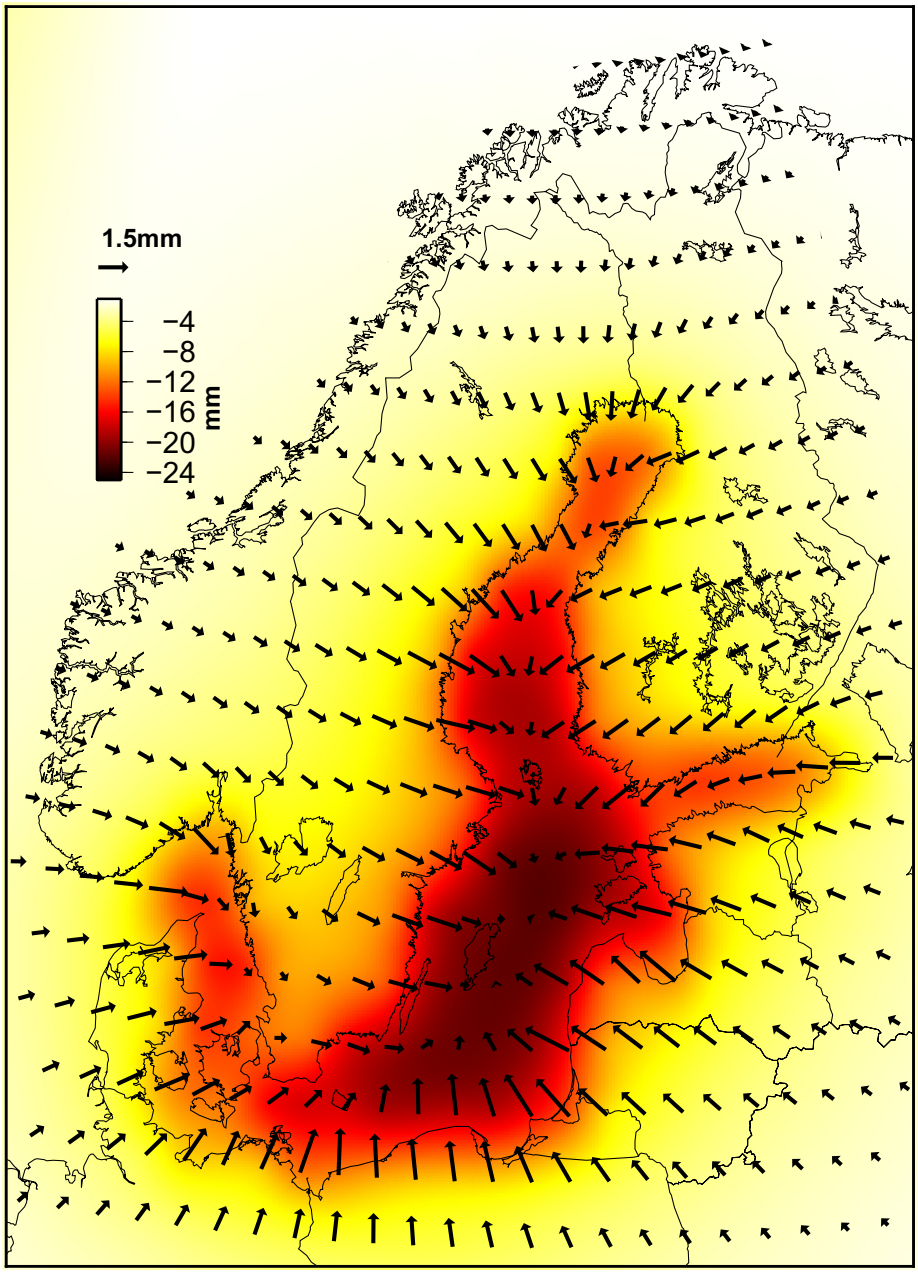

Fig. 1. The 3D deformation due to one meter of water in the whole of the Baltic Sea.

transformation to ITRF2008 we just fixed one point at its ITRF2008 coordinates. The network orientation comes from the IGS08 orbits used. The data span of these time series is February 2008 until March 2010, but due to some data gaps the last ten months have been left out. Thus, the time series length is 480 days, starting February 2008, ending in May 2009.

Both time series use IERS conventions [16,22] for the solid Earth tides (IERS2003 and IERS2010 for FGI and JPL, respectively) and ocean tidal loading parameters from FES2004 ocean tide model. JPL daily position estimates are in IGS08, which is aligned to ITRF2008, FGI daily positions are in ITRF2008. Cut-off angle is 3° in the FGI time series and 15° in the JPL time series. Both time series refer to center of figure of the Earth (CF) frame. For a discussion of the CF and CE reference frames (and the CM frame which we do not use) see Blewitt [5], Argus [3], and Wu et al. [30]. The small difference between the CF frame of the coordinate time series and the CE frame of the load time series is near-completely eliminated when forming coordinate differences and load differences in the limited area.

The FES2004 ocean tide model includes the Baltic Sea. The Baltic Sea tides are thus removed from the GNSS positions but included in the modelled Baltic load (see Section 2.1). We will return to this inconsistency in Section 5.

Vectors were formed between station pairs, and the variation of the vector transformed to north, east and up (NEU) components. As the vectors are relatively short, we neglect the non-parallelity of the NEU components at the two ends.

The FGI time series was originally produced with very little data screening. Consequently, outlier rejection had to be performed, with two-sigma deviation from the mean as a criterion. If any of the three NEU components was rejected by this criterion, all three components were discarded. The JPL time series had already been edited by the producers, and a lighter screening using three-sigma was sufficient.

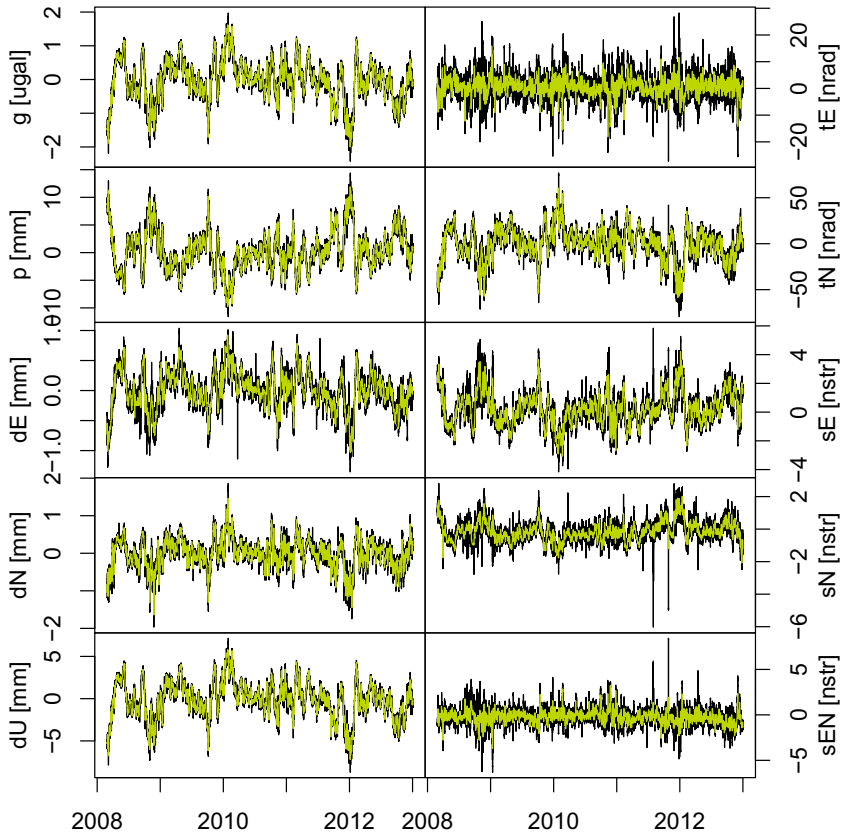

Fig. 2. Time series of modelled 3D deformation due to non-tidal loading by the Baltic Sea, for station Metsähovi (METS). Black is hourly time series, green is daily. The variables: (from top left) gravity (microgal), potential divided by normal gravity (millimetre), deformation in east, north and up (millimetre), (from top right) tilt in east and north (nanoradian), strain in east, north and shear strain (nanostrain).

4. Results

Fig. 3 shows the positions of stations we used in the comparisons in Fig. 4 and Tables 1 and 2. Fig. 4 shows the GPS time series and the computed 3D loading for the pair Visby–Metsähovi (VIS0-METS).

For the sample station pair VIS0-METS seen in Fig. 4, the visual compatibility of difference loading and position time series is good. The load time series seem to capture both long-period variation and also some shorter variations in the GPS time series. Especially the east component shows high similarity.

The good fit in the east component turns out to be a general feature of the data. We have computed the standard deviation of the north, east and up components for some station pairs (stations named in Fig. 4) before and after the Baltic loading has been corrected for. The results are shown for JPL time series in Table 1 and for FGI time series in Table 2.

The good performance of the load correction for the east component, 6 out of 7 (Table 1) and 7 out of 8 (Table 2) are improved, in both the JPL and FGI time series obviously depends on the fact that most vectors have one end east of the Baltic and the other west of the Baltic. The load will then influence the ends with a different sign.

For the north component we in most cases do not have similar amplification of the correction, 4 out of 7 (Table 1) and 7 out of 8 (Table 2) are improved. This is visible in the size of the corrections (columns "North bs") and it can also be guessed from Fig. 1. Even so, the FGI time series show consistent improvement. Regarding the up component, 4 out of 7 (Table 1) and 6 out of 8 (Table 2) are improved, in many cases a large part of it is eliminated in differencing as both stations are close to the coast. But even when the correction is large (the four last FGI vectors, Table 2, Up) it fails to produce an appreciable improvement in the GPS variance.

For the JPL time series, both north and up component show more erratic behaviour w.r.t. the corrections. Interestingly, though, for the only vector (VIS0-METS) that is present both in the JPL and FGI time series, the improvements from load are very similar. That they are percentually less in the JPL series is mostly due to the larger noise to start with.

The Baltic level and thus our load corrections are correlated with atmospheric pressure which we have not corrected for. We have therefore performed a diagnostic calculation where we have regressed the GNSS time series on the load corrections, instead of making a simple subtraction as in Tables 1 and 2. The diagnostics failed to reveal any hidden correlations. Where Tables 1 and 2 show that the load correction provides an improvement, the regression generally gave it a coefficient near unit value, and where the load correction provides no improvement in Tables 1 and 2 the regression gives it a coefficient near zero (results not shown).

To demonstrate an extremely high reduction in standard deviation we have picked a 100 day period from east component of MAR6-OLKI (FGI solution, Fig. 5). The reduction in variance is 54%. Adding a 3-day filter for both time series increases the reduction in variance to 65%. Test runs however show that using the filtering for the longer time series does not give reductions as large as this, so the good fit in the 100 day interval could be fortuitous.

5. Discussion

We have conducted a preliminary study on how the non-tidal variation in Baltic Sea load is distinguishable in time series of GPS-derived coordinates. In order to attenuate the common-mode

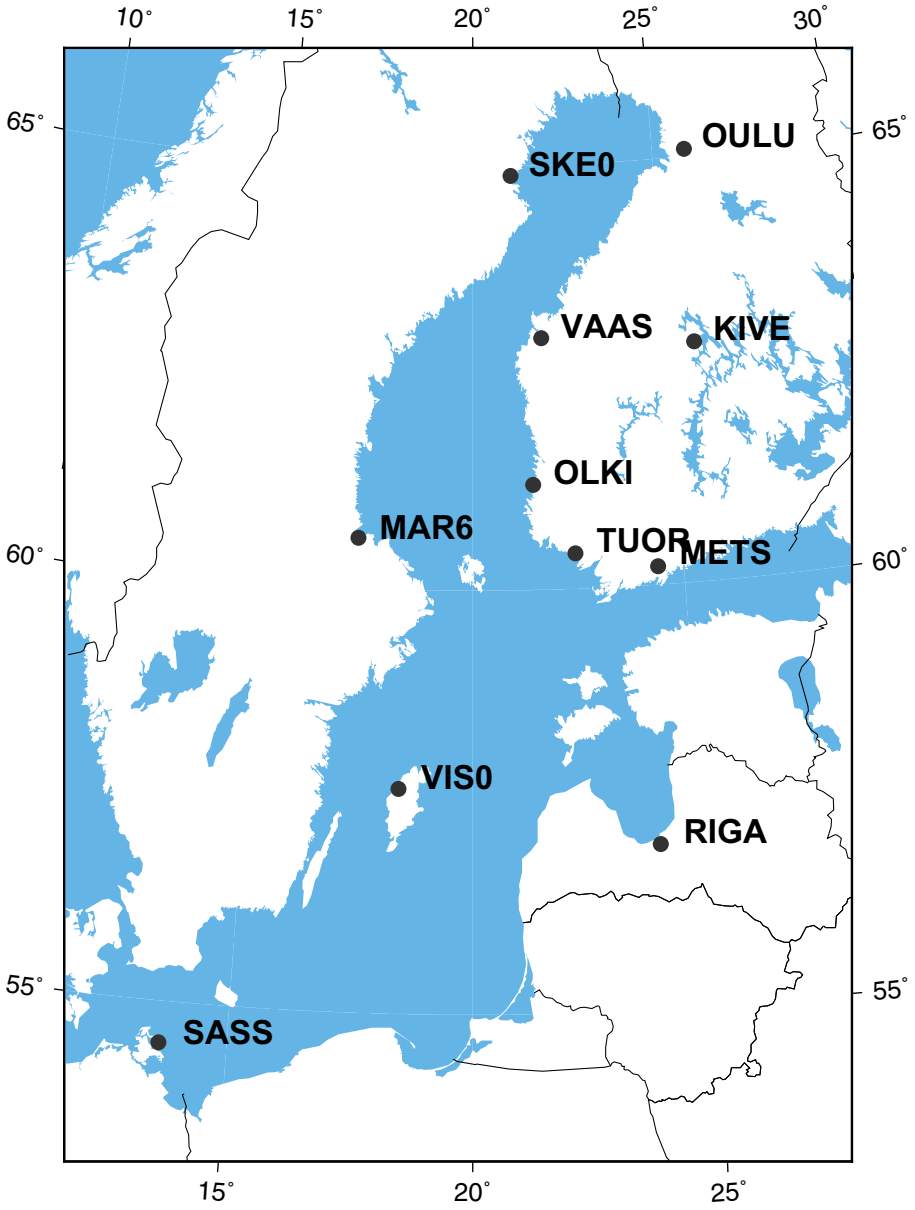

Fig. 3. Map showing the position of the GPS stations used in the comparison. The used station pairs are listed in Tables 1 and 2.

type effects of other load signals in the GPS time series we formed differences of both coordinates and of modelled load for station pairs. The results are encouraging: the Baltic load is well detectable. The loading shows in the east component most prominently. The up component shows some signal as well as the north component. The atmospheric loading affects the up component the most, requiring a more detailed study on the subject. In our previous study [19] the atmospheric loading correction did not reduce the standard deviation at any station, whereas van Dam et al. [24] and Jiang et al. [14] find reductions.

Our previous study [19] showed the effect of environmental effects, including Baltic Sea, on monthly time scales on the vertical GPS time series. In that study, with different GPS time series, different time spans and different corrections and their combinations gave very different reductions to the standard deviation. This is true also for the present study, even for only Baltic Sea, shown by the varying reduction percentages from site to site, using different GPS time series and different time series length.

The storm surge study by Geng et al. [13] yields reductions in standard deviation of up to 28% in up component and up to 13% in horizontal components for a 2-hourly time series over a month. Their reduction depends on the site and its distance from the shore. During the extremes GPS and the deformation agree nicely, which can be seen also in our daily time series.

van Dam et al. [24] found the scatter of their time series to diminish at 65% of the studied stations when non-tidal ocean loading was corrected for. Their reductions were up to 0.7 mm in the weekly vertical time series, which compares well with our range (from zero up to 1 mm) of reductions in the up component, although the results are not directly comparable due to different atmospheric handling.

Our results point at several issues that will be addressed in follow-up studies. First and foremost, we will include the atmospheric loading computation. Then, our use of observations (tide gauge data) instead of models to approximate the Baltic load brings both problems and benefits. The smooth sea level surface

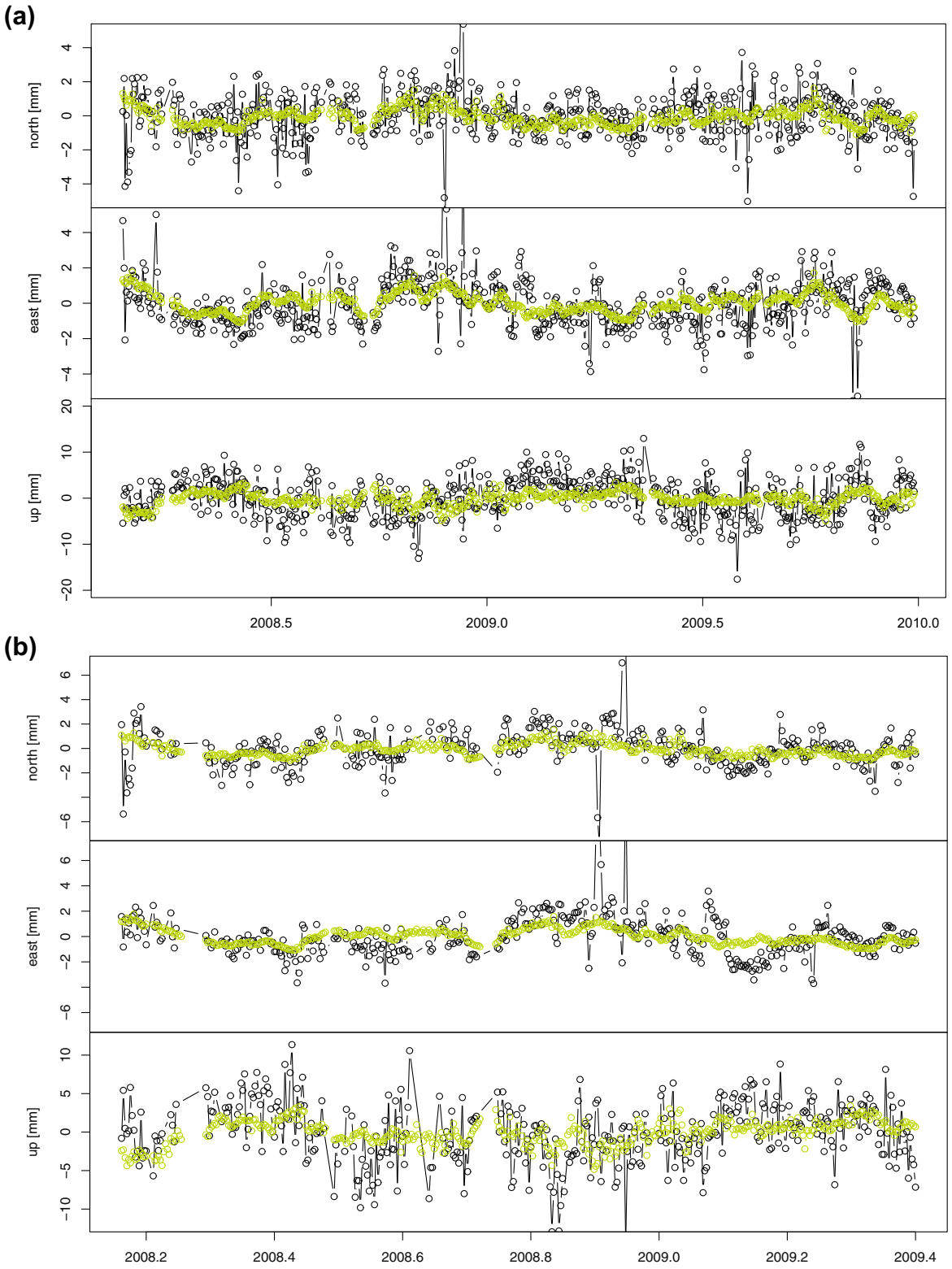

Fig. 4. Three components of difference position time series from GPS (before outlier rejection) and difference loading time series for station pair VIS0-METS from (a) JPL time series and (b) FGI time series. GPS time series are in black and loading is in green. Note the difference in the scales.

interpolated from tide gauges does not account for ocean dynamics and may suffer e.g. from coastal effects. Also, the steric effects will need to be imported from models in any case.

On the other hand, even the high-resolution regional Baltic models currently in operative use show sea level prediction errors of several centimetres, as can be verified from the web pages of the institutions producing these predictions. For best accuracy a reanalysis and/or assimilation of observations would be needed. Of course, the question is whether all this makes any difference at all for the load calculations given the accuracy of the geodetic observations to be corrected. Here it should be pointed out that while we here treat GPS observations only, in the same project

Table 1
The JPL time series standard deviation (sd), loading time series standard deviation (bs), the standard deviation after loading correction (sd–bs) in millimetres and the percentage of variance explained by the loading correction (%) for north, east and up component. Length of the time series is 671 days. Trend was first removed from all the time series.

Vector	North				East				Up			
	sd	bs	sd–bs	%	sd	bs	sd–bs	%	sd	bs	sd–bs	%
VIS0-METS	1.41	0.49	1.32	12	1.34	0.55	1.16	25	4.02	1.46	3.77	12
MAR6-VAAS	1.81	0.19	1.84	−3	1.76	0.97	1.42	35	7.34	0.54	7.27	2
MAR6-METS	1.86	0.34	1.77	10	1.83	0.94	1.71	13	4.05	0.47	4.09	−2
VIS0-SASS	1.26	0.48	1.23	−4	1.13	0.36	1.17	−8	4.67	1.93	4.89	−10
VIS0-VAAS	1.72	0.34	1.83	−13	1.47	0.59	1.22	32	7.29	1.92	7.14	4
MAR6-RIGA	1.69	0.56	1.64	7	1.80	1.11	1.67	15	4.93	0.60	4.96	−1
VIS0-RIGA	1.40	0.45	1.32	12	1.16	0.75	0.90	39	4.84	1.65	4.50	14

Table 2
The FGI time series standard deviation (sd), loading time series standard deviation (bs), the standard deviation after loading correction (sd–bs) in millimetres and the percentage of variance explained by the loading correction (%) for north, east and up component. The length of the time series is 480 days. Trend was first removed from all the time series.

Vector	North				East				Up			
	sd	bs	sd–bs	%	sd	bs	sd–bs	%	sd	bs	sd–bs	%
MAR6-TUOR	1.27	0.36	1.21	9	1.55	1.02	1.10	50	3.07	0.47	3.14	−5
MAR6-OLKI	0.98	0.20	0.96	3	1.40	1.17	0.93	56	3.23	0.74	3.22	1
SKE0-OULU	0.86	0.22	0.87	6	0.93	0.82	0.86	16	3.24	0.61	3.22	1
SKE0-KIVE	0.91	0.25	0.87	9	0.85	0.59	0.70	32	3.51	0.68	3.60	−5
SKE0-OLKI	1.25	0.31	1.20	7	1.06	0.89	0.86	34	3.55	1.31	3.38	9
VIS0-OLKI	1.36	0.35	1.36	0	0.94	0.63	0.96	−4	4.63	2.61	4.37	11
VIS0-TUOR	1.09	0.49	0.95	23	1.12	0.60	0.94	30	3.24	1.17	3.05	12
VIS0-METS	1.18	0.48	0.98	31	1.26	0.54	1.05	31	3.51	1.45	3.21	16

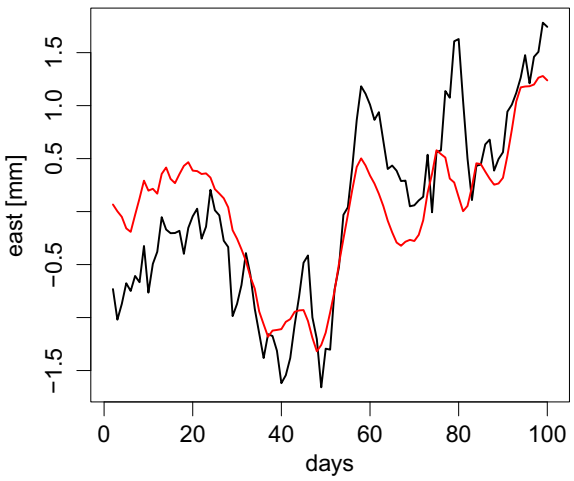

Fig. 5. A three month period (starting 14.3.2009) for east component of MAR6-OLKI. Black is GPS and red is loading. A linear filter has been used to reduce the scatter of GPS time series.

we are also producing gravity predictions (Fig. 2) for a much more sensitive instrument, the superconducting gravimeter at Metsähovi [25].

As mentioned in Sections 2.1 and 3, the hourly sea surfaces interpolated from the tide gauges contain the Baltic tides, though in an approximate way, i.e. by assuming that they can be smoothly interpolated between tide gauges. At the same they are removed from the GPS-derived coordinates using the FES2004 model. The Baltic load tides are not quite negligible; for instance in METS (Fig. 3) the amplitude of the M2 load tide from the FES2004 is 0.13 mm in the Up component and the amplitude of the K1 load tide 0.08 mm in the East component. However, in the present case the inconsistency in the treatment of the load and in the treatment of the GPS-derived coordinates is negligible: we average the load over 24 h and then the contribution of diurnal and semidiurnal tides to it is much attenuated and will mostly show up as longer-period aliases. Nevertheless, in some other applications of the tide-gauge derived loading it will be necessary to reconcile it with load-tide corrections from ocean tide models.

One more aspect of the tide-gauge derived loading deserves to be explored. In this paper we have used it primarily for demonstrating the concept. However, we may envisage long-term correction series for all geodetic quantities in the Baltic region. In such long-term series the stability of the reference will be important, in order not to introduce e.g. spurious trends into the corrected geodetic data. In a tide-gauge derived loading the geodetic definition and maintenance of the reference is straightforward as the majority of tide gauges are nowadays continuously monitored with geodetic methods and, e.g. their post-glacial rebound rates have been determined.

At present, though, the situation with the real-time BOOS and FMI data we used in this paper is the opposite. The data are relative to national mean sea level definitions and references and thus vary from country to country and from year to year. For the present purposes the effects of these shortcomings are negligible. The data are traceable to geodetic references and the shortcomings will be fixed in future studies.

6. Conclusions and outlook

We have computed time series of non-tidal loading due to the Baltic Sea. The time series have been computed altogether for 193 stations in northern Europe. In this study we have compared the modelled Baltic Sea loading to GNSS time series with two different computation techniques. We have compared station pairs to better reveal the movements, especially on the opposite sides of the Baltic basin. The results show that Baltic Sea level variation induced vertical and horizontal movements are visible in daily GPS time series. When correcting for the Baltic Sea loading, the variance of time series reduces by up to 56% in the East component and up to 30% and 16% in North and Up, respectively. The reduction depends on the station pair.

In future computations we will use controlled sea level surface data, instead of real-time, and apply a common and controlled reference level. This is especially important in trend derivations.

We will include the steric effect and also compare our sea level surfaces to regional and global ocean models. The atmospheric loading effect will be taken into account. The time series will be extended back and forward in time.

The computed loading time series for the 193 stations are available from the corresponding author.

Acknowledgements

The tide gauge data providers (BOOS and FMI) are kindly acknowledged. We would also like to thank the two anonymous reviewers for their comments. The figures were created using programs GMT [27] and R [23].

References

[1] Agnew DC. SPOTL: Some programs for the ocean-tide loading, Scripps Institution of Oceanography Technical Report, available at <http://escholarship.org/uc/item/954322pg>; 2012.
[2] Antonov JI, Seidov D, Boyer TP, Locarnini RA, Mishonov AV, Garcia HE et al. World Ocean Atlas 2009: Salinity, NOAA Atlas NESDIS 69; 2010. p. 184.
[3] Argus DF. Uncertainty in the velocity between the mass center and surface of Earth. J Geophys Res 2012;117(B10):B10405.
[4] Bertiger W, Desai S, Haines B, Harvey N, Moore A, Owen S, Weiss J. Single receiver phase ambiguity resolution with GPS data. J Geodyn 2010;84:327–37.
[5] Blewitt G. Self-consistency in reference frames, geocenter definition, and surface loading of the solid Earth. J Geophys Res 2003;108(B2):2103. doi: 2110.1029/2002JB002082.
[6] Blewitt G, Lavallée D. Effect of annual signals on geodetic velocity. J Geophys Res 2002;107:B72145. http://dx.doi.org/10.1029/2001JB000570.
[7] Collilieux X, van Dam T, Ray J, Coulot D, Métivier L, Altamimi Z. Strategies to mitigate aliasing of loading signals while estimating GPS frame parameters. J Geodyn 2012;86:1–14. http://dx.doi.org/10.1007/s00190-011-0487-6.
[8] Dach R, Hugentobler U, Fridez P, Meindl M, editors. Bernese GPS Software, Version 5.0. Astronomical Institute, University of Berne; 2007.
[9] Dong D, Fang P, Bock Y, Cheng MK, Miyazaki S. Anatomy of apparent seasonal variations from GPS-derived site position time series. J Geophys Res 2002;107. http://dx.doi.org/10.1029/2001JB000573.
[10] Ekman M. A consistent map of the postglacial uplift of Fennoscandia. Terra Nova 1996;8:158–65.
[11] Farrell WE. Deformation of the Earth by surface loads. Rev Geophys Space Phys 1972;10:761–97.
[12] Fratepietro F, Baker TF, Williams SDP, Van Camp M. Ocean loading deformations caused by storm surges on the northwest European shelf. Geophys Res Lett 2006;33:L06317. http://dx.doi.org/10.1029/2005GL025475.
[13] Geng JSDP, Williams FN. Teferle and A.H. Dodson, 2012, Detecting storm surge loading deformations around the southern North Sea using subdaily GPS. Geophys J Int 2012;191:569–78. http://dx.doi.org/10.1111/j.1365-246X.2012.05656.x.
[14] Jiang W, Li Z, van Dam T, Ding W. Comparative analysis of different environmental loading methods and their impacts on the GPS height time series. J Geodesy 2013;87(7):687–703.
[15] Mathers EL, Woodworth PL. Departures from the local inverse barometer model observed in altimeter and tide gauge data and in a global barotropic numerical model. J Geophys Res C 2002;106:6957–72. http://dx.doi.org/10.1029/2000JC000241.
[16] McCarthy D, Petit G. IERS Conventions (IERS Technical Note; 32) Frankfurt am Main: Verlag des Bundesamts für Kartographie und Geodäsie; 2004. p. 127, paperback. ISBN: 3-89888-884-3.
[17] Mémin A, Watson C, Haigh ID, MacPherson L, Tregoning P. Non-linear motions of Australian geodetic stations induced by non-tidal ocean loading and the passage of tropical cyclones. J Geodesy 2014;88:927–40. http://dx.doi.org/10.1007/s00190-014-0734-8.
[18] Munekane H, Matsuzaka S. Nontidal ocean mass loading detected by GPS observations in the tropical Pacific region. Geophys Res Lett 2004;31. http://dx.doi.org/10.1029/2004GL019773.
[19] Nordman M, Mäkinen J, Virtanen H, Johansson J, Bilker-Koivula M, Virtanen J. Crustal loading in vertical GPS time series in Fennoscandia. J Geodyn 2009;48:144–50. doi: 101.1016/j.jog.2009.09.003.
[20] Novotny K, Liebsch G, Lehmann A, Dietrich R. Variability of sea surface heights in the Baltic Sea: an intercomparison of observations and model simulations. Mar Geodesy 2006;29(2):113–34.
[21] Olsson P-A, Scherneck H-G, Ågren J. Effects on gravity from nontidal sea level variations in the Baltic Sea. J Geodyn 2009;48:151–6. http://dx.doi.org/10.1016/j.jog.2009.09.002.
[22] Petit G, Luzum B, editors. IERS Conventions (IERS Technical Note; 36) Frankfurt am Main: Verlag des Bundesamts für Kartographie und Geodäsie; 2010. p. 179, ISBN: 3-89888-989-6.
[23] R Development Core Team 2010. R: A language and environment for statistical computing. R Foundation for Statistical Computing, Vienna, Austria. ISBN 3-900051-07-0, URL http://www.R-project.org/.
[24] van Dam TX, Collilieux X, Wuite J, Altamimi Z, Ray J. Nontidal ocean loading: amplitudes and potential effects in GPS height time series. J Geodyn 2012. http://dx.doi.org/10.1007/s00190-012-0564-5.
[25] Virtanen H. Studies of earth dynamics with the superconducting gravimeter [PhD dissertation]. University of Helsinki; 2006 (available at http://ethesis.helsinki.fi/).
[26] Virtanen J, Mäkinen J, Koivula-Bilker M, Virtanen H, Nordman M, Kangas A, et al. Baltic sea mass variations from GRACE: comparison with in situ and modelled sea level heights. In Proceedings of the International Symposium Gravity, Geoid and Earth Observation, International Association of Geodesy Symposia; 2009.
[27] Wessel P, Smith WHF. New, improved version of generic mapping tools released. EOS Trans. AGU 1998;79(47):579. http://dx.doi.org/10.1029/98EO00426.
[28] Wiehl M, Dietrich R, Lehmann A. How Baltic Sea water mass variations mask the postglacial rebound signal in CHAMP and GRACE gravity field solutions. In: Reigber C, Lühr H, Schwintzer P, Wickert J, editors. Earth observation with CHAMP. Results from three years in orbit, Springer; 2005. p. 181–86.
[29] Williams SDP, Penna NT. Non-tidal ocean loading effects on geodetic GPS heights. Geophys Res Lett 2011;38:L09314. http://dx.doi.org/10.1029/2011GL046940.
[30] Wu X, Ray J, van Dam T. Geocenter motion and its geodetic and geophysical implications. J Geodyn 2012;58:44–61. http://dx.doi.org/10.1016/j.jog.2012.01.007.
[31] Wunsch C, Stammer D. Atmospheric loading and the oceanic "inverted barometer" effect. Rev Geophys 1997;31:79–107.
[32] Zumberge JF, Heflin MB, Jefferson DC, Watkins MM, Webb FH. Precise point positioning for the efficient and robust analysis of GPS data from large networks. J Geophys Res 1997;102(B3):5005–17.